An Adaptive MTPA Control Method Based on Improved EKO for PMa-SynRM Drive System

Jiang Lin, Haoran Qin, Xiaosong He, Jixiang Cheng and Cunyong Qiu

October 23, 2023

An Adaptive MTPA Control Method based on improved EKO for PMa-SynRM Drive System

Lin Jiang *
School of Electrical Engineering and Information, Southwest Petroleum University
Cheng Du, China
e-mail: jlin57@163.com

Haoran Qin
School of Electrical Engineering and Information, Southwest Petroleum University
Cheng Du, China
e-mail: 1048299875@qq.com

Xiaosong He
School of Electrical Engineering and Information, Southwest Petroleum University
Cheng Du, China
e-mail: 2998997131@qq.com

Jixiang Cheng
School of Electrical Engineering and Information, Southwest Petroleum University
Cheng Du, China
e-mail: Chengjixiang0106@126.com

Cunyong Qiu
School of Electrical Engineering and Information, Southwest Petroleum University
Cheng Du, China
e-mail: chaucer@swpu.edu.cn

***Abstract*—The maximum torque per ampere (MTPA) control is usually used to achieve optimal control of energy efficiency of electric vehicles (EVs). However, the MTPA control strategy depends heavily on the motor model and parameters. The EVs are affected by temperature change, magnetic saturation and other factors during operation, which will lead to deterioration of MTPA control performance. Therefore, an adaptive MTPA control method based on improved extended Kalman observer (EKO) for permanent-magnet assisted synchronous reluctance motor (PMa-SynRM) drive system is proposed. By establishing the equivalent model of PMa-SynRM with iron loss, an improved extended Kalman filter algorithm based on d-axis current zeroing is proposed. This algorithm can estimate the iron loss and inductance parameters of the motor on the line, and the MTPA control parameters can be corrected in real time to optimize the stator current vector. The simulation results show that the proposed method has fast convergence speed, high parameter identification accuracy, and improves the MTPA control performance in case of parameter mismatch.**

Keywords- Maximum torque per ampere (MTPA), permanent magnet assisted synchronous reluctance motor (PMa-SynRM), extended Kalman observer (EKO), parameter identification

I. INTRODUCTION

PMa-SynRM has gradually become a cost reduction and efficiency enhancement solution in the field of electric vehicles due to its high saliency ratio and low rare earth materials content [1]. During the working of PMa-SynRM, the stator resistance, d-q axis inductance, and flux amplitude will change due to factors such as temperature rise and magnetic saturation, which will affect the MTPA control effect [2,3]. Therefore, studying online identification of inductance parameters and adaptive adjustment of MTPA controller parameters is an effective means to improve the performance of PMa-SynRM drive systems.

The series of Kalman Filter (KF) algorithms are widely used in solving practical engineering problems [4-7]. Extended Kalman Filter (EKF) algorithm is used for real-time identification of interior permanent magnet synchronous motor (IPMSM) inductance in [8], and a Dual Kalman Filter algorithm is proposed for real-time identification of IPMSM inductance in [9], but neither of them consider the impact of iron loss on inductance identification. To accurately identify the iron loss equivalent resistance of a motor, a Dual Extended Kalman Filter algorithm is proposed in [10], which can simultaneously obtain the state and convergence estimation of the iron loss equivalent resistance. However, the design of the algorithm does not consider changes in other parameters. The method of using fundamental pulse width modulation excitation and current derivative measurement to expand the rank of the motor nonlinear system matrix can achieve simultaneous identification of motor iron loss and inductance [11], but this identification algorithm has severe parameter coupling and is relatively complex.

To simplify the identification of iron loss and inductance parameters in PMa-SynRM, an improved Extended Kalman observer (EKO) based on d-axis current zeroing is proposed. Improving EKO by adding iron loss correction factors to the state transition matrix of the motor, using the d-axis current zeroing method to identify the equivalent resistance value of the motor iron loss in real time, calculating and updating the iron loss correction factors, achieving high-precision and fast dynamic response inductance parameter identification, and optimizing the MTPA controller parameters.

II. MATHEMATICAL MODEL OF PMA-SYNRM WITH IRON LOSS

The structure of PMa-SynRM is shown in Figure 1, with a larger saliency ratio compared to IPMSM, and the q-axis inductance value is more susceptible to current changes and magnetic circuit saturation.

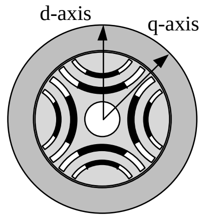

Fig. 1. Structure of PMa-SynRM

Motor iron loss is the phenomenon of iron core heating caused by the continuous flipping and friction of internal magnetic domains of ferromagnetic materials under the action of alternating magnetic fields. The power of an equivalent iron loss resistance can be used to simulate the heat loss power of the iron core [12]. The d-q axis equivalent circuits of PMa-SynRM are shown in Figure 2.

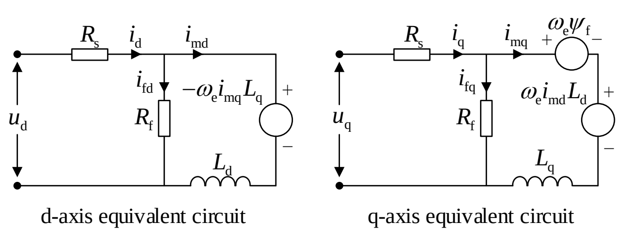

Fig. 2. Equivalent circuits of PMa-SynRM

The electromagnetic relationship of PMa-SynRM can be described as:

$$i_d = i_{md} + \frac{L_d \dfrac{di_{md}}{dt} - \omega_e i_{mq} L_q}{R_f} \tag{1}$$

$$i_q = i_{mq} + \frac{L_q \dfrac{di_{mq}}{dt} + \omega_e i_{md} L_d + \omega_e \psi_f}{R_f} \tag{2}$$

$$\frac{di_{md}}{dt} = \frac{u_d - i_d R_s + \omega_e i_{mq} L_q}{L_d} \tag{3}$$

$$\frac{di_{mq}}{dt} = \frac{u_q - i_q R_s - \omega_e i_{md} L_d - \omega_e \psi_f}{L_q} \tag{4}$$

where u_d and u_q are the stator voltage components of d and q-axis, i_d and i_q are the stator current components of d and q-axis, i_{md} and i_{mq} are the torque current components of d and q-axis, i_{fd} and i_{fq} are the iron loss current components of d and q-axis, L_d and L_q are the inductance components of d and q-axis, R_s is the stator resistance, R_f is the equivalent iron loss resistance, ω_e is the electrical angular velocity, and Ψ_f is the amplitude of the permanent magnet flux.

The rotor motion equation of the motor is:

$$J \frac{d\omega_m}{dt} = T_e - T_L - B\omega_m \tag{5}$$

The torque equation is:

$$T_e = \frac{3}{2} n_p \left[\psi_f i_{mq} + \left(L_d - L_q \right) i_{md} i_{mq} \right] \tag{6}$$

where T_e is the electromagnetic torque, T_L is the load torque, n_p is the number of motor poles, ω_m is the mechanical angular velocity, J is the moment of inertia, and B is the rotor viscosity coefficient.

Under MTPA control, the current relationship of the d-q axis is:

$$\begin{cases} i_d = \dfrac{-\psi_f + \sqrt{\psi_f^2 + 8(L_d - L_q)^2 i_s^2}}{4(L_d - L_q)} \\ i_q = \sqrt{i_s^2 - i_{dt}^2} \end{cases} \tag{7}$$

III. IRON LOSS PARAMETER IDENTIFICATION OF PMA-SYNRM

According to the PMa-SynRM electromagnetic torque equation (6), when the motor rotates in the forward direction, the q-axis current must be greater than zero, while the d-axis current can be equal to zero within a certain torque and speed range.

The principle of the d-axis current zeroing method is shown in Figure 3. At moment A, the iron loss parameter identification is activated, MTPA control is interrupted, the d-axis current value is set to zero, the q-axis current value is adjusted by the speed loop PID controller, and at moment B, the motor returns to MTPA control to complete the iron loss parameter identification. The difference between i_d and i_{md} is the d-axis iron loss current component. The value of i_d is known, but the value of i_{md} is unknown, so calculating the value of i_{md} is a necessary condition for calculating the equivalent resistance of iron loss.

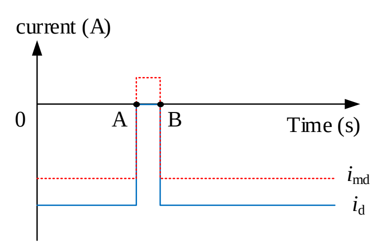

Fig. 3. Schematic diagram of d-axis current zero setting method

The relationship between motor torque and electrical angular velocity is:

$$\begin{cases} T_e = \dfrac{3}{2} n_p \psi_f \sqrt{\dfrac{u_s^2 - \omega_e^2 \psi_f^2}{\omega_e^2 L_q^2}} \\ u_s^2 = u_d^2 + u_q^2 \end{cases} \tag{8}$$

When controlling the motor with i_d=0, it is necessary to ensure that the intersection point of the voltage limit circle and the current limit circle on the q-axis is not lower than the intersection point of the torque curve on the q-axis.

When the d-axis current is set to zero and the constraint relationship in equation (8) is met, the d-axis inductance of the motor is the nominal value. At this point, the d-axis iron loss current value is equal to the negative d-axis torque current value, the equivalent resistance of iron loss can be calculated:

$$\begin{cases} i_{\mathrm{md}} = \dfrac{u_{\mathrm{q}} - R_{\mathrm{s}} i_{\mathrm{q}} - \omega_{\mathrm{e}} \psi_{\mathrm{f}} - L_{\mathrm{q}} \dfrac{\mathrm{d}i_{\mathrm{mq}}}{\mathrm{d}t}}{-\omega_{\mathrm{e}} L_{\mathrm{d}}} \\ R_{\mathrm{f}} = \dfrac{L_{\mathrm{d}} \dfrac{\mathrm{d}i_{\mathrm{md}}}{\mathrm{d}t} + u_{\mathrm{d}}}{i_{\mathrm{md}}} \end{cases} \tag{9}$$

The stator resistance value and permanent magnet flux value in equation (9) are mainly affected by temperature and can be obtained by other means; The differential term of torque current cannot be directly measured, and the stator current differential term can be used instead of the torque current differential term:

$$\frac{\mathrm{d}i_{\mathrm{md}}}{\mathrm{d}t} = \frac{\mathrm{d}i_{\mathrm{d}}}{\mathrm{d}t} \;, \quad \frac{\mathrm{d}i_{\mathrm{mq}}}{\mathrm{d}t} = \frac{\mathrm{d}i_{\mathrm{q}}}{\mathrm{d}t} \tag{10}$$

Due to the fact that the amplitude of L_q value is much lower than other terms, its variation has minimal impact on the calculation of i_{md}. Therefore, the nominal value of L_q can be used to calculate the equivalent resistance of iron loss.

IV. Improved EKO Inductance Parameter Identification

EKO is a parameter observer with EKF as the core algorithm. To address the identification error caused by neglecting iron loss in traditional EKO, the iron loss correction factors are added to the motor state transition matrix in EKO, which is called Improved EKO.

The nonlinear equation of the system is:

$$\frac{\mathrm{d}}{\mathrm{d}t}\begin{bmatrix} i_{\mathrm{d}} \\ i_{\mathrm{q}} \\ a \\ b \end{bmatrix} = \begin{bmatrix} a\left(u_{\mathrm{d}} - R_{\mathrm{s}} i_{\mathrm{d}}\right) + \dfrac{a}{b}\left(\omega_{\mathrm{e}} i_{\mathrm{q}} - \lambda_{\mathrm{q}} - \delta_{\mathrm{q}}\right) \\ b\left(u_{\mathrm{q}} - R_{\mathrm{s}} i_{\mathrm{q}} - \omega_{\mathrm{e}} \psi_{\mathrm{f}}\right) - \dfrac{b}{a}\left(\omega_{\mathrm{e}} i_{\mathrm{d}} - \lambda_{\mathrm{d}} + \delta_{\mathrm{d}}\right) \\ 0 \\ 0 \end{bmatrix} \tag{11}$$

Selecting system state variables:

$$x = \begin{bmatrix} i_{\mathrm{d}} & i_{\mathrm{q}} & a & b \end{bmatrix}^{\mathrm{T}} \tag{12}$$

where $a = \dfrac{1}{L_{\mathrm{d}}}$, $b = \dfrac{1}{L_{\mathrm{q}}}$, $\lambda_{\mathrm{d}} = \dfrac{u_{\mathrm{d}}\omega_{\mathrm{e}}}{R_{\mathrm{f}}}$, $\lambda_{\mathrm{q}} = \dfrac{u_{\mathrm{q}}\omega_{\mathrm{e}}}{R_{\mathrm{f}}}$, $\delta_{\mathrm{d}} = \dfrac{R_{\mathrm{s}} i_{\mathrm{d}} \omega_{\mathrm{e}}}{R_{\mathrm{f}}}$, $\delta_{\mathrm{q}} = \dfrac{R_{\mathrm{s}} i_{\mathrm{q}} \omega_{\mathrm{e}}}{R_{\mathrm{f}}}$, λ_d, λ_q, δ_d and δ_q are iron loss correction factors.

The output variables are:

$$y = \begin{bmatrix} i_{\mathrm{d}} & i_{\mathrm{q}} \end{bmatrix}^{\mathrm{T}} \tag{13}$$

Discretize equation (11) by the forward difference method to obtain the state transition matrix A and output matrix H as follows:

$$A = \begin{bmatrix} 1 - T_{\mathrm{s}} a R_{s} & T_{\mathrm{s}}\left(\dfrac{a}{b}\omega_{\mathrm{e}} - \dfrac{\delta_{\mathrm{q}}}{i_{\mathrm{q}}}\right) & A_{13} & A_{14} \\ -\dfrac{T_{\mathrm{s}} b}{a}\left(\omega_{\mathrm{e}} + \dfrac{\delta_{\mathrm{d}}}{i_{\mathrm{d}}}\right) & 1 - T_{\mathrm{s}} b R_{\mathrm{s}} & A_{23} & A_{24} \\ 0 & 0 & 1 & 0 \\ 0 & 0 & 0 & 1 \end{bmatrix} \tag{14}$$

$$H = \begin{bmatrix} 1 & 0 & 0 & 0 \\ 0 & 1 & 0 & 0 \end{bmatrix} \tag{15}$$

where $A_{13} = T_{\mathrm{s}} u_{\mathrm{d}} - T_{\mathrm{s}} R_{\mathrm{s}} i_{\mathrm{d}} + \dfrac{T_{\mathrm{s}}}{b}\left(\omega_{\mathrm{e}} i_{\mathrm{q}} - \lambda_{\mathrm{q}} - \delta_{\mathrm{q}}\right)$,

$$A_{14} = \frac{T_{\mathrm{s}} a}{b^2}\left(\lambda_{\mathrm{q}} + \delta_{\mathrm{q}} - \omega_{\mathrm{e}} i_{\mathrm{q}}\right),$$

$$A_{23} = \frac{T_{\mathrm{s}} b}{a^2}\left(\omega_{\mathrm{e}} i_{\mathrm{d}} - \lambda_{\mathrm{d}} + \delta_{\mathrm{d}}\right),$$

$$A_{24} = T_{\mathrm{s}} u_{\mathrm{q}} - T_{\mathrm{s}} R_{\mathrm{s}} i_{\mathrm{q}} - T_{\mathrm{s}} \omega_{\mathrm{e}} \psi_{\mathrm{f}} - \frac{T_{\mathrm{s}}}{a}\left(\omega_{\mathrm{e}} i_{\mathrm{d}} - \lambda_{\mathrm{d}} + \delta_{\mathrm{d}}\right).$$

V. Simulation Experiments

To verify the feasibility and accuracy of the proposed inductance and iron loss identification method, a PMa-SynRM control model is constructed as shown in Figure 4. Among them, the improved EKO error covariance matrix P=diag ([0.1 0.1 10 10]), the output observation noise covariance matrix Q=diag ([1 1 10000 10000]), and the input observation noise covariance matrix R=diag ([1 1]).

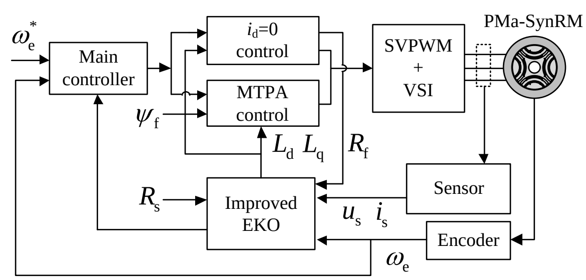

Fig. 4. PMa-SynRM control structure block diagram

The initial simulation parameters are shown in Table I.

TABLE I. SIMULATION PARAMETERS OF PMA-SYNRM

parameter	value
Rated power (P_N / kW)	8
Stator resistance (R_s / Ω)	0.2
Iron loss resistance (R_f / Ω)	40
d-axis inductance (L_d / mH)	0.5
q-axis inductance (L_q / mH)	1.63
Permanent magnetic linkage (ψ_m / Wb)	0.197
pole pair (n_p)	3
moment of inertia (J /kg·m^2)	0.017
Viscosity coefficient (B / Nm s/rad)	0.008
switching frequency (f_S / Hz)	10000
Rated voltage (U_N / V)	300

A. *Improved EKO identification effect under variable working conditions*

To simulate changes in the working conditions of PMa-SynRM drive system, the simulation parameters of the motor drive system are designed as follows:

The initial reference speed is 1000 r/min, and the load torque is 40 N·m. The load torque changes to 30 N·m at 2 seconds. At 3 seconds, reference speed suddenly changes to 1500 r/min. At 4 seconds, due to temperature changes and magnetic circuit saturation, the d-axis inductance changes from the nominal value of 0.5 mH to 0.51 mH, and the q-axis inductance changes from the nominal value of 1.63 mH to 1.32 mH. At 6 seconds, the magnetic flux amplitude decreases by 20% from 0.197 Wb to 0.1576 Wb due to temperature changes. At 8 seconds, the d-axis inductance further changes to 0.52 mH, with a total change rate of 4%, and the q-axis inductance changes to 1.01 mH, with a total change rate of 38%. The simulation runs until 10 seconds.

The identification results of equivalent resistance of iron loss and the amplitude of rotor flux are shown in Figure 5. The identification value of rotor magnetic flux is mainly affected by sudden changes in motor working conditions, and the identification value of iron loss equivalent resistance is mainly affected by sudden changes in speed and magnetic flux. When the magnetic flux amplitude changes from 0.197 Wb to 0.1576 Wb, the iron loss resistance identification curve converges to stability after 118ms, and the accurate iron loss equivalent resistance value of 40 Ω is identified.

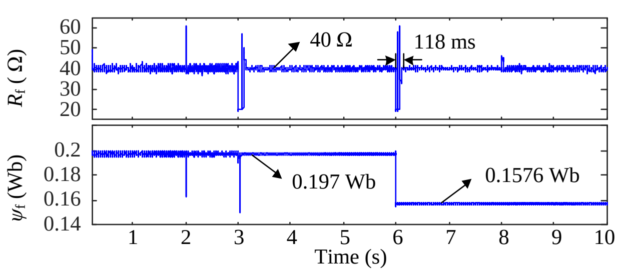

Fig. 5. Amplitude of R_f and Ψ_f

The comparison of inductance identification effects between improved EKO and traditional EKO is shown in Figure 6. The inductance parameters identified by improved EKO are more accurate compared to traditional EKO, and the identification value of inductance has a fast dynamic response speed; The changes in speed and rotor flux cause jitter in the inductance identification waveform. After a sudden change in speed, the identification results of the d-axis inductance converged to stability after 163ms, and the identification results of the q-axis inductance converged to stability after 157ms. After a sudden change in the rotor flux amplitude, the d-axis inductance identification results converged to stability after 114ms, and the q-axis inductance identification results converged to stability after 127ms. The inductance value identified by improved EKO accurately follows the actual value.

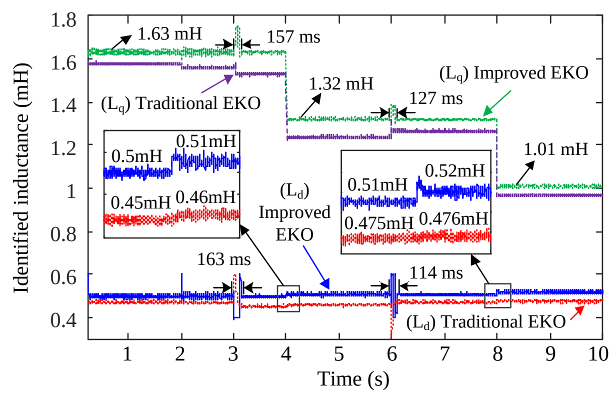

Fig. 6. Effect of inductance identification

The comparison of inductance identification errors between improved EKO and traditional EKO is shown in Figure 7. The maximum d-axis inductance error identified by traditional EKO is 9.6%, and the maximum q-axis inductance error identified is 6.01%. The identification error of d-axis inductance and q-axis inductance in the improved EKO algorithm is almost zero, and the identification accuracy is significantly improved.

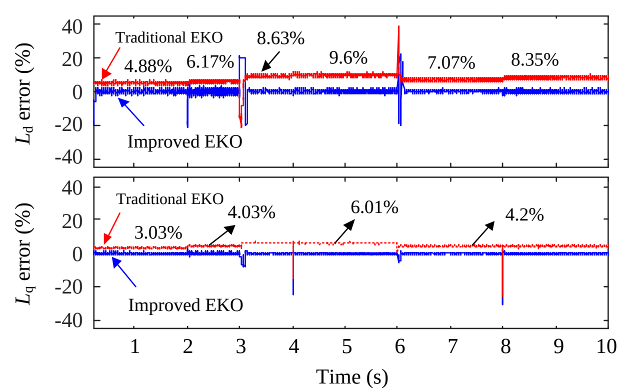

Fig. 7. Inductance identification error curve

B. The control effect of Improved EKO combined with MTPA

To verify the compatibility of the proposed improved EKO and MTPA control method, the simulation results are shown in Figure 8.

After the motor starts, the iron loss identification algorithm is activated at 0.4 seconds, MTPA control is restored at 0.6 seconds, iron loss identification algorithm is activated again at 1.4 seconds, MTPA control is restored at 1.6 seconds, and simulation operation ends at 2 seconds.

By utilizing the characteristics of rapid convergence in identification of d-axis inductance and iron loss equivalent resistance, the controller briefly sets the d-axis current to zero according to demand, quickly identifies and records the d-axis inductance and iron loss equivalent resistance, and adopts MTPA control method for the rest of the time.

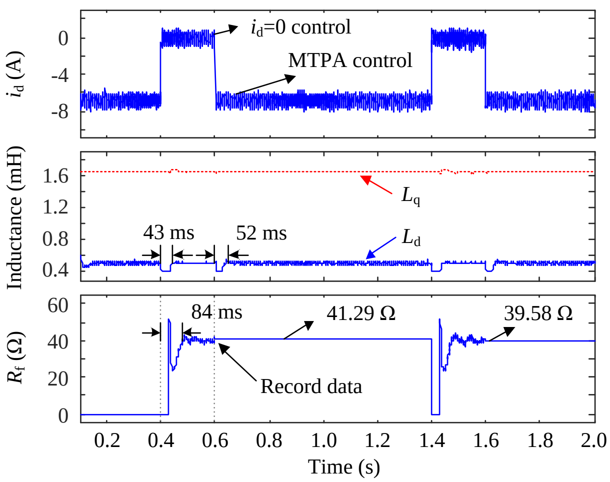

Fig. 8. Effect of parameter identification algorithm

As shown in the figure, after the iron loss identification algorithm is turned on, the identification value of the equivalent resistance of the iron loss converges to stability after 84ms, and the identification value of the d-axis inductance converges to stability after 43ms. The identification of the q-axis inductance is almost unaffected by the switching of control modes; After the iron loss identification algorithm is turned off, the d-axis inductance identification value converges to stability again after 52ms, and the controller maintains the last recorded iron loss equivalent resistance data, which is 41.29 Ω for the first time and 39.58 Ω for the second time.

C. Adaptive MTPA control optimization effect

To verify the improvement of the adaptive MTPA control effect based on improved EKO, the motor speed was set at 1000 r/min, and the load torque varied from 40 N · m to 10 N · m. The stator current angle and vector amplitude were observed. Figure 9 compares the current angle between adaptive MTPA control and traditional MTPA control under changing operating conditions.

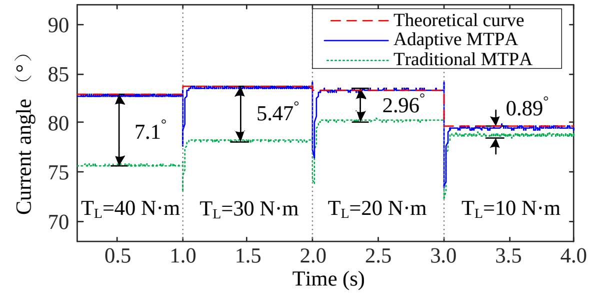

Fig. 9. Comparison of stator current angle

The stator current angle controlled by adaptive MTPA accurately tracks the theoretical current angle curve, while the stator current angle controlled by traditional MTPA deviates from the theoretical current angle curve, and the larger the load torque, the greater the angle deviation.

The data in Table II compares the amplitude of stator current vector of adaptive MTPA control and traditional MTPA control.

TABLE II. COMPARISON OF STATOR CURRENT VECTOR AMPLITUDES

Load torque	The amplitude of i_s		Optimization rate
	Adaptive MTPA	***Traditional MTPA***	
10 N·m	13.00A	14.51A	10.4%
15 N·m	18.50A	19.99A	7.45%
20 N·m	23.96A	25.34A	5.45%
25 N·m	29.34A	30.84A	4.86%
30 N·m	34.69A	36.46A	4.85%
35 N·m	39.99A	41.55A	3.75%
40 N·m	45.27A	46.87A	3.41%

From the table, it can be seen that under different load torque conditions, the amplitude of stator current vector of adaptive MTPA is smaller than that of traditional MTPA, and the smaller the load torque, the better the optimization effect.

VI. CONCLUSION

This article combines PMa-SynRM working conditions to propose an adaptive MTPA method based on d-axis current zeroing to identify the equivalent resistance of iron loss, and using improved EKO to update inductance parameters online. This improves the accuracy of motor inductance parameter identification and solves the problem of inductance identification error caused by iron loss in traditional EKO, furthermore, the problem of deteriorating control performance of the motor MTPA controller due to mismatched inductance parameters in the presence of iron loss was solved. The simulation results show that the proposed method has the characteristics of high parameter identification accuracy, fast dynamic response, simple algorithm design, good compatibility, and strong robustness.

ACKNOWLEDGMENT

This work is part of the "Study on efficiency optimization control strategy of new permanent magnet assisted reluctance motor drive system for electric vehicles". And it is supported by Chengdu Science and Technology Foundation No. 2022-YF05-00157-SN.

REFERENCES

[1] Muteba M. "Surface-Mounted V-shapes PM assisted-Synchronous Reluctance Motor for Light Electric Vehicles," 2022 IEEE Transportation Electrification Conference & Expo (ITEC). IEEE, 2022: 409-413.

[2] Neumann J, Hénaux C, Fadel M, et al. "Improved dq model and analytical parameters determination of a Permanent Magnet Assisted Synchronous Reluctance Motor (PMa-SynRM) under saturation using frozen permeability method,"2020 International Conference on Electrical Machines (ICEM). IEEE, 2020, 1: 481-487.

[3] Shi W , Zhou X . "Online Estimation Method for Permanent Magnet Temperature of High‐Density Permanent Magnet Synchronous Motor," IEEJ Transactions on Electrical and Electronic Engineering, 2020, 15(5).

[4] Nair D S, Jagadanand G, George S. "Torque estimation using kalman filter and extended kalman filter algorithms for a sensorless direct torque controlled bldc motor drive: a comparative study," Journal of Electrical Engineering & Technology, 2021, 16(5): 2621-2634.

[5] Zhang H W, Jiang D, Wang X H, et al. "Direct Torque Sensorless Control of PMSM Based on Dual Extended Kalman Filter," 2021 33rd Chinese Control and Decision Conference (CCDC). IEEE, 2021: 7499-7504.

[6] Zerdali E . "A Comparative Study on Adaptive EKF Observers for State and Parameter Estimation of Induction Motor," IEEE Transactions on Energy Conversion, 2020.

[7] Cui J, Xing W, Qin H, et al. "Research on Permanent Magnet Synchronous Motor Control System Based on Adaptive Kalman Filter," Applied Sciences, 2022, 12(10): 4944.

[8] Sim H W, Lee J S, Lee K B. "On-line parameter estimation of interior permanent magnet synchronous motor using an extended Kalman filter," Journal of Electrical Engineering and Technology, 2014, 9(2): 600-608.

[9] Zwerger T , Mercorelli P . "A Dual Kalman Filter to Identify Parameters of a Permanent Magnet Synchronous Motor," 2020 24th International Conference on System Theory, Control and Computing (ICSTCC). 2020.

[10] Li J , Nie S F , Meng Q L , et al. "Efficiency optimization of induction motors based on online identification of iron loss equivalent resistance via dual extended Kalman filter," 2016 IEEE Region 10 Conference (TENCON). IEEE, 2017.

[11] Mynar Z , Vaclavek P , Blaha P . "Synchronous Reluctance Motor Parameter and State Estimation Using Extended Kalman Filter and Current Derivative Measurement," IEEE Transactions on Industrial Electronics, 2020, PP(99):1-1.

[12] Hang J, Wu H, Ding S, et al. "Improved loss minimization control for IPMSM using equivalent conversion method," IEEE Transactions on Power Electronics, 2020, 36(2): 1931-1940.